

Anisotropy Scaling Functions in Heavy-Ion Collisions: Insights into the ‘Ultra-Central Flow Puzzle’ and Constraints on Transport Coefficients and Nuclear Deformation

Roy A. Lacey^{1,*}

¹Department of Chemistry, Stony Brook University,
Stony Brook, NY, 11794-3400, USA

(Dated: February 15, 2024)

Anisotropy scaling functions, derived from extensive measurements of transverse momentum- and centrality-dependent anisotropy coefficients $v_2(p_T, \text{cent})$ and $v_3(p_T, \text{cent})$ in Pb+Pb collisions at 5.02 and 2.76 TeV, and Xe+Xe collisions at 5.44 TeV at the LHC, shed light on the ‘ultra-central flow puzzle’. These functions amalgamate diverse measurements into a unified curve, elucidating anisotropy attenuation across the full p_T and centrality range and unveiling dependencies on key factors including initial-state eccentricities (ε_n), dimensionless size (\mathbb{R}), radial flow, viscous correction to the thermal distribution function (δ_f), the medium’s stopping power (\hat{q}), and specific shear viscosity (η/s). Their analysis provides distinct insights into transport coefficients and nucleus deformation constraints.

PACS numbers: 25.75.-q, 25.75.Dw, 25.75.Ld

Azimuthal anisotropy measurements play a crucial role in the ongoing research aimed at determining the temperature (T) and baryon chemical potential (μ_B) dependence of the transport coefficients of the quark gluon plasma (QGP) produced in heavy ion collisions at the Relativistic Heavy Ion Collider (RHIC) and the Large Hadron Collider (LHC). These measurements are commonly quantified as a function of collision centrality (cent) and particle transverse momentum p_T using the complex coefficients [1–3]:

$$V_n \equiv v_n e^{in\Psi_n} = \langle e^{in\phi} \rangle, \quad (1)$$

where v_n characterizes the magnitude of the azimuthal anisotropy of the particle spectrum in the plane transverse to the beam direction, Ψ_n is the event-plane and the single brackets denote an average with respect to the single-particle spectrum in a collision event.

The v_n coefficients are related to the Fourier coefficients v_{nn} , which characterize the amplitude of two-particle correlations in relative azimuthal angle $\Delta\phi = \phi_i - \phi_j$ for particles i and j, forming pairs [4, 5]:

$$\frac{dN^{pairs}}{d\Delta\phi} \propto 1 + 2 \sum_{n=1}^{\infty} v_{nn} \cos(n\Delta\phi),$$

$$v_{nn}(p_T^i, p_T^j) = v_n(p_T^i)v_n(p_T^j) + \delta_{NF}, \quad (2)$$

where δ_{NF} signifies possible non-flow contributions that are often mitigated with experimental cuts[5–8].

Mechanistically, the coefficients v_n are linked to the underlying dynamics of collective flow for $p_T \lesssim 4 – 5$ GeV, transitioning to jet quenching at larger p_T . This linkage is substantiated by an extensive body of research [9–40] indicating that v_n is influenced by factors such as radial expansion, v_n -fluctuations, p_T -dependent viscous attenuation, jet quenching, and the shape of the initial-state anisotropic density profile $\rho(r, \varphi)$ in the transverse (\perp) plane of the colliding nuclei. This shape is effectively characterized by complex eccentricity co-

efficients [21, 41–44]:

$$\varepsilon_n \equiv \varepsilon_n e^{in\Phi_n} = \frac{\int d^2r_{\perp} r^m e^{in\varphi} \rho(r, \varphi)}{\int d^2r_{\perp} r^m \rho(r, \varphi)}, \quad (3)$$

where r and φ are the radius and the azimuthal angle and Φ_n represents the angle associated with the n^{th} -order participant plane ($m = n$ for $n \geq 2$ and $m = 3$ for $n = 1$) [17, 21, 45, 46]. The deformed Woods-Saxon distribution,

$$\rho(r, \theta, \varphi) = \frac{\rho_0}{1 + \exp\left(\frac{r - R(\theta, \varphi)}{a}\right)}, \quad (4)$$

$$R(\theta, \varphi) = R_0 \{1 + \beta_2 [\cos \gamma Y_{20}(\theta, \varphi) + \sin \gamma Y_{22}(\theta, \varphi)]\},$$

is frequently employed to model the nucleon configurations of non-spherical nuclei. Here, ρ_0 denotes the central nuclear density, R_0 parametrizes the nuclear radius and a is the nuclear skin thickness. The spherical harmonics Y_{lm} , along with the coefficients β_2 and γ encode the shape of the nucleus. Specifically, β_2 quantifies the magnitude of deformation while γ , varying between $\gamma = 0$ and $\gamma = 60^\circ$, indicates the degree of asymmetry in the nucleus’s shape. The event-by-event fluctuations in the initial state density profile lead to corresponding fluctuations in ε_n .

Dynamical models based on relativistic hydrodynamics indicate an approximate linear mapping $v_n \propto \varepsilon_n$ [46–48], and have demonstrated success in capturing both the magnitude and trend of v_n coefficients [15, 21, 31, 49–52]. These models have also played a pivotal role in ongoing attempts to constrain the transport properties of the QGP through Bayesian inference [53–60]. However, a significant challenge arises as these models fall short of simultaneously describing v_2 and v_3 data in ultra-central collisions (cent $\lesssim 1\%$) [61]. Specifically, either the calculated v_2 is larger than measured, or the predicted v_3 is too small, or a combination of both inconsistencies exists.

The puzzling discrepancy in hydrodynamic models’ inability to simultaneously describe v_2 and v_3 in ultra-central collisions challenges conventional expectations. The anticipation

was that these models would excel in central collisions, given the anticipated increase in charge particle multiplicities ($\langle N_{\text{chg}} \rangle$) and volumes of locally thermalized domains. This incongruity introduces uncertainty, questioning whether these extensively employed models might lack essential ingredients necessary for constraining the initial state and transport coefficients.

Despite numerous dedicated efforts to solve the enigmatic “ultra-central flow puzzle” by refining initial conditions [62–70], investigating the influence of transport coefficients [62, 64, 71, 72], and exploring the role of equations of state [73], a definitive solution to this puzzle has remained elusive.

This work investigates a resolution to the puzzle based on anisotropy scaling functions constructed using detailed measurements of $v_2(p_T, \text{cent})$ and $v_3(p_T, \text{cent})$ in collisions of 5.02 and 2.76 TeV Pb+Pb and 5.44 TeV Xe+Xe at the LHC. The insights gained from these scaling functions suggest that a nuanced consideration of anisotropy attenuation holds promise for unraveling the puzzle. Furthermore, these functions provide distinctive constraints for transport coefficients, eccentricity spectra, and the initial-state deformation of the Xe nucleus.

In this study, we employ the concept of anisotropy scaling functions, which is based on the idea that a diverse set of measurements for $v_2(p_T, \text{cent})$ and $v_3(p_T, \text{cent})$ can be unified into a single curve, aptly termed the scaling function. This unification relies on the consideration of specific parameters influencing $v_n(p_T, \text{cent})$, including the initial-state eccentricities (ε_n), dimensionless size ($RT = \mathbb{R}$), radial flow magnitude, the medium’s stopping power (\hat{q}), and its specific shear viscosity or viscosity-to-entropy ratio ($\eta/s \propto T^3/\hat{q}$) [74], as well as the viscous correction to the thermal distribution function (δ_f) [13].

Consequently, we can succinctly express the anisotropy coefficients driven by the flow using Eq. 5 [34, 75–77]:

$$v_n(p_T, \text{cent}) = \varepsilon_n e^{-\frac{\beta}{\mathbb{R}}[n(n+\kappa p_T^2)]}, \quad n = 2, 3, \quad (5)$$

where $\beta \propto \eta/s$, $\delta_f = \kappa p_T^2$ [13, 34], and $\mathbb{R} \propto \langle N_{\text{chg}} \rangle_{|\eta| \leq 0.5}^{1/3}$ is related to the mid-rapidity ($|\eta| \leq 0.5$) charged particle multiplicity. The transition from flow coefficients to those for jet quenching at higher p_T is achieved seamlessly by requiring a consistency between η/s and \hat{q} that ensures a smooth merge of the low and high momentum regions of δ_f [13]. This transition is facilitated by fixing the κp_T^2 term in Eq. 5 to a constant value for p_T above the cut (typically around 4.5 GeV/c), which serves as the threshold distinguishing the flow-dominated and jet quenching domains.

Equation 5 reveals a crucial insight: In the domain of the most central collisions, characterized by the peak value \mathbb{R}_0 , a scaling connection emerges. This equation links the observed values of the harmonic $v_n(p_T, 0)$ in these ultra-central events with those observed as $v_n(p_T, \text{cent})$ at different centralities, each tied to its corresponding \mathbb{R}' value:

$$\frac{v_n(p_T, 0)}{v_n(0)} e^{\frac{n\beta}{\mathbb{R}_0}(n+\kappa p_T^2)} = \left(\frac{v'_n(p_T, \text{cent})}{\varepsilon'_n(\text{cent})} \right) e^{\frac{n\beta}{\mathbb{R}_0}(n+\kappa p_T^2)(\frac{\mathbb{R}_0}{\mathbb{R}} - 1)}, \quad (6)$$

where the exponential on the left-hand side of the equation accounts for the anisotropy attenuation in ultra-central collisions, and that on the right-hand side accounts for the relative attenuation at other centralities.

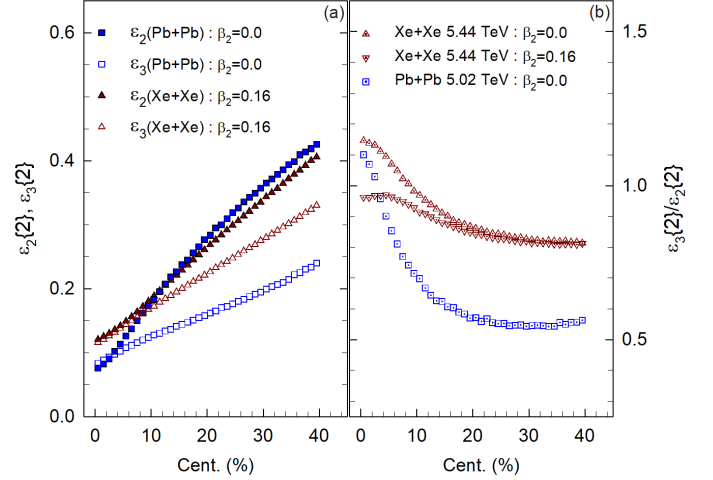


FIG. 1. (Color Online) Panel (a) contrasts the centrality-dependent values of ε_2 and ε_3 for 5.02 TeV Pb+Pb collisions featuring spherical Pb nuclei and 5.44 TeV Xe+Xe collisions characterized by deformed Xe+Xe nuclei. In panel (b), the ratios $\varepsilon_3/\varepsilon_2$ are compared for spherical Pb nuclei ($\beta_2 = 0$) and both spherical and deformed Xe nuclei, as indicated.

Moreover, when preserving a fixed centrality within a given system, a revealing correlation emerges between the values of $v_2(p_T, \text{cent})$ and $v_3(p_T, \text{cent})$. These values, both subject to the same influences of radial flow, η/s , and \hat{q} , adhere to the following relationship:

$$\frac{v_2(p_T, \text{cent})}{v_2(\text{cent})} e^{\frac{2\alpha\beta}{\mathbb{R}_0}} = \left(\frac{v_3(p_T, \text{cent})}{v_3(\text{cent})} \right)^{\frac{2}{3}}, \quad (7)$$

where α represents a system-dependent (yet centrality-independent) normalizing constant. Equations 6 and 7 encapsulate the intricate dependencies of the high and low p_T anisotropy coefficients from ultra-central to peripheral collisions, underlining that the scaled values of $v_2(p_T, \text{cent})$ and $v_3(p_T, \text{cent})$ measurements can be effectively collapsed onto a single curve or scaling function S_{FS} . Therefore, the identification of such scaling functions would furnish compelling evidence for the coherence of the scaling coefficients and the trustworthiness of the corresponding eccentricity spectrum and its ratios.

The eccentricity ratio is of paramount importance due to its nuanced dependence on centrality and deformation, as depicted in Fig. 1. This figure presents the calculated values of ε_2 , ε_3 , and their ratio for both Pb+Pb and Xe+Xe collisions at energies of 5.02 TeV and 5.44 TeV, revealing distinctive dependencies. These dependencies not only constrain the respective eccentricity spectrum but also provide insights into the initial-state deformation of the Xe nucleus, underscoring

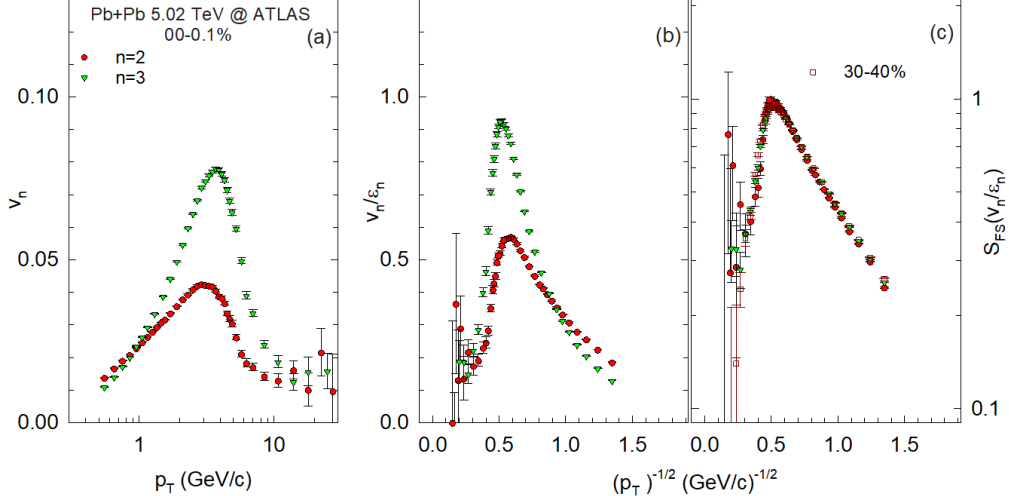


FIG. 2. (Color Online) Comparison of $v_2(p_T)$ and $v_3(p_T)$ in panel (a), their eccentricity-scaled values v_2/ε_2 and v_3/ε_3 in panel (b), and the resulting scaling function in panel (c) for 0.1% central Pb+Pb collisions at 5.02 TeV. Panel (c) also includes scaled results for 30-40% central Pb+Pb collisions. The data are sourced from the ATLAS collaboration [78].

the critical role of central collisions in quantifying this deformation.

The data utilized in this study are sourced from the ATLAS [8, 78] and ALICE [79, 80] collaborations, encompassing $v_2(p_T, \text{cent})$ and $v_3(p_T, \text{cent})$ measurements for Pb+Pb collisions at $\sqrt{s_{NN}} = 2.76$ and 5.02 TeV, as well as Xe+Xe collisions at 5.44 TeV. The required centrality-dependent $\langle N_{\text{chg}} \rangle_{|\eta| \leq 0.5}$ values were derived from corresponding multiplicity density measurements [81–84]. We adopted the previously established value $\kappa = 0.17$ (GeV/c) $^{-2}$ [34] to compute δf . The eccentricities were computed according to the procedure outlined in Eq. 3, with the assistance of a Monte Carlo quark-Glauber model (MC-qGlauber) featuring fluctuating initial conditions [34]. This model, based on the widely used MC-Glauber model [85, 86], accounts for the finite size of the nucleon, the nucleon’s wounding profile, the distribution of quarks within the nucleon, and quark cross sections that accurately reproduce the NN inelastic cross section for the corresponding beam energies. Calculations were performed for spherical Pb nuclei and Xe nuclei with varying degrees of initial-state deformation characterized by $\gamma = 0$ and several different values for the β_2 parameter (cf. Eq. 4). A systematic uncertainty of 2-3% was estimated for the eccentricities based on variations in the model parameters.

Scaling functions were derived from differential measurements of $v_2(p_T, \text{cent})$ and $v_3(p_T, \text{cent})$ for Pb+Pb collisions at 2.76 and 5.02 TeV, as well as Xe+Xe collisions at 5.44 TeV, employing Eqs. 6 and 7. The \mathbb{R}_0 value for ultra-central Pb+Pb collisions at 5.02 TeV served as the reference. Figure 2 demonstrates the scaling procedure for 0.1% central Pb+Pb collisions at 5.02 TeV, utilizing $1/\sqrt{p_T}$ for the x-axis in panels (b) and (c) to accentuate the flow- and jet-quenching-dominated domains. Panel (a) underscores the disparity be-

tween the values of $v_2(p_T)$ and $v_3(p_T)$, while panel (b) indicates that eccentricity scaling ($v_2(p_T)/\varepsilon_2$ and $v_3(p_T)/\varepsilon_3$) alone fails to account for their difference. Panel (c) presents the resulting scaling function, demonstrating data convergence onto a single curve for both p_T domains, providing robust evidence for the consistency of the scaling coefficients and the validity of the corresponding eccentricity spectrum and its ratios. Validation of the scaling function spanned the entire measurement range (0.0-0.1% to 50-60%) for $\beta = 0.88$ and $\alpha = 1$, as demonstrated in Figure 3 for the $v_2(p_T, \text{cent})$ measurements. The attenuation factor for the 0-5% centrality cut reflects an average that incorporates values from both ultra-central and non-ultra-central collisions, given that this selection encompasses contributions from both. Similarly, a robust scaling function, nearly identical to that for Pb+Pb collisions at 5.02 TeV, was obtained across the full range of measurements for Pb+Pb collisions at 2.76 TeV, with $\beta = 0.84$ and $\alpha = 1.25$, suggesting an approximate 5% relative decrease in η/s when the collision energy is reduced from 5.02 to 2.76 TeV.

The observed scaling function, which spans both domains for flow and jet-quenching with identical scaling coefficients, lends further support to the conjecture proposed by Majumder et al. [74] that η/s and T^3/\hat{q} are related. This scaling behavior, particularly the dependence of high p_T anisotropy on the dimensionless size $\mathbb{R} \propto \langle N_{\text{chg}} \rangle^{1/3}$, confirms their reliance on path length and suggests a significant role of radiative energy loss in driving these jet-quenching-induced anisotropy coefficients. Additionally, the observation of a seamless transition between low and high momentum regions of δf at the p_T threshold distinguishing the flow and jet-quenching domains provides a crucial constraint for the relative magnitude of η/s and T^3/\hat{q} [13]. This magnitude difference serves as a vital parameter for distinguishing between a strongly-coupled and

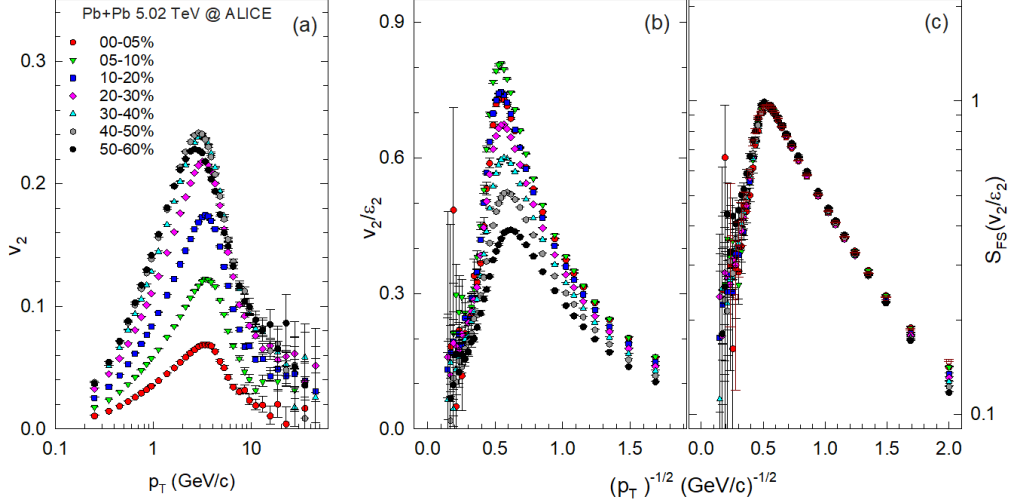


FIG. 3. (Color Online) Comparison of $v_2(p_T)$ in panel (a), their eccentricity-scaled values (v_2/ε_2) in panel (b), and the resulting scaling function in panel (c) for various centralities in Pb+Pb collisions at 5.02 TeV. Data sourced from the ALICE collaboration [79].

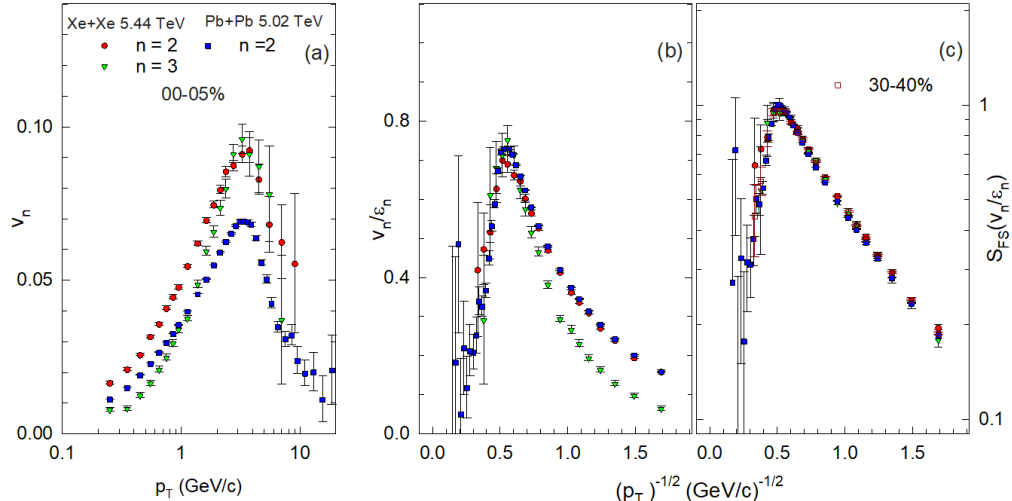


FIG. 4. (Color Online) Comparison of the $v_2(p_T)$ and $v_3(p_T)$ values for Xe+Xe collisions and $v_2(p_T)$ for Pb+Pb collisions in panel (a), their eccentricity-scaled values v_2/ε_2 and v_3/ε_3 in panel (b), and the resulting scaling function in panel (c) for 0-5% central collisions. Panel (c) also includes scaled results for 30-40% central Xe+Xe collisions. The data are sourced from the ALICE collaboration [79, 80].

weakly-coupled quark-gluon plasma [74]. A rudimentary estimate, following the formalism for δf in Ref. [13] and by requiring consistency between η/s and \hat{q} to ensure a smooth merge of the low and high momentum regions of δf , indicates $\eta/s > T^3/\hat{q}$, suggesting a strongly coupled plasma.

The scaling function provides unique insights into nuclear deformation, as previously illustrated in Fig. 1 and summarized in Fig. 4. In the latter figure, we compare the $v_2(p_T)$ and $v_3(p_T)$ results for Xe+Xe collisions with the $v_2(p_T)$ results for Pb+Pb collisions for the 0-5% centrality cut, utilizing the eccentricities for the deformed Xe nucleus ($\beta_2 = 0.16$ [87]). Panel (a) highlights a significant difference between $v_2(p_T)$ and $v_3(p_T)$ for Xe+Xe collisions, reflecting the expected vari-

ation in viscous attenuation for the two harmonics. These values exhibit notably larger magnitudes than those of $v_2(p_T)$ for Pb+Pb collisions, consistent with the larger eccentricities determined for Xe+Xe collisions (cf. Fig. 1). Panel (b) shows that while eccentricity scaling cannot fully account for the $v_2(p_T) - v_3(p_T)$ difference in panel (a), it effectively explains the considerable difference between the $v_2(p_T)$ data for Xe and Pb in the same panel. Panel (c) presents the resulting scaling function, revealing data collapse onto a single curve for both flow- and jet-quenching-dominated domains, providing compelling evidence for the coherence of the scaling coefficients and the reliability of the corresponding eccentricity spectrum for the deformed Xe nucleus. The validation of

the scaling function extends across the full range of centrality measurements (0-5% to 40-50%) for $\beta = 0.90$, $\alpha = 0$, $\beta_2 = 0.16$. Larger or smaller values of β_2 result in less robust scaling functions, indicating deformed Xe nuclei and only an approximate 2% relative increase in η/s when the beam energy is raised from 5.02 TeV to 5.44 TeV. Further detailed comparisons with Pb+Pb collisions at various centralities suggest slightly larger relative radial flow in 5.02 TeV Pb+Pb collisions than in 5.44 TeV Xe+Xe collisions. Notably, the utilization of scaling functions for studying nuclear deformation offers a significant advantage by (i) reliably accounting for the anisotropy attenuation in central collisions and (ii) relying on the measurement of $v_2(p_T)$ and $v_3(p_T)$ in identical events within the same system. This approach leads to substantial reductions in systematic uncertainties from various sources.

In summary, anisotropy scaling functions, derived from extensive measurements of $v_2(p_T, \text{cent})$ and $v_3(p_T, \text{cent})$ in Pb+Pb collisions at 5.02 and 2.76 TeV, and Xe+Xe collisions at 5.44 TeV, provide crucial insights into the ‘ultra-central flow puzzle’ and constrain transport coefficients, the eccentricity spectrum, and nucleus deformation. Consolidating diverse measurements into a single curve, these functions account for specific parameters influencing $v_n(p_T, \text{cent})$, including initial-state eccentricities (ε_n), dimensionless size (\mathbb{R}), radial flow magnitude, the medium’s stopping power (\hat{q}), and its specific shear viscosity (η/s), as well as the viscous correction to the thermal distribution function (δ_f). They yield distinct constraints for transport coefficients and nucleus deformation.

ACKNOWLEDGEMENT

This research is supported by the US DOE under contract DE-FG02-87ER40331.A008.

* E-mail: Roy.Lacey@Stonybrook.edu

- [1] A. Bilandzic, R. Snellings, and S. Voloshin, *Phys. Rev.* **C83**, 044913 (2011), arXiv:1010.0233 [nucl-ex].
- [2] M. Luzum, *J. Phys.* **G38**, 124026 (2011), arXiv:1107.0592 [nucl-th].
- [3] D. Teaney and L. Yan, *Phys. Rev.* **C86**, 044908 (2012), arXiv:1206.1905 [nucl-th].
- [4] A. M. Poskanzer and S. A. Voloshin, *Phys. Rev.* **C58**, 1671 (1998), arXiv:nucl-ex/9805001 [nucl-ex].
- [5] R. A. Lacey, *Proceedings, 18th International Conference on Ultra-Relativistic Nucleus-Nucleus Collisions (Quark Matter 2005): Budapest, Hungary, August 4-9, 2005*, *Nucl. Phys.* **A774**, 199 (2006), arXiv:nucl-ex/0510029 [nucl-ex].
- [6] M. Luzum and J.-Y. Ollitrault, *Phys. Rev. Lett.* **106**, 102301 (2011), arXiv:1011.6361 [nucl-ex].
- [7] E. Retinskaya, M. Luzum, and J.-Y. Ollitrault, *Phys. Rev. Lett.* **108**, 252302 (2012), arXiv:1203.0931 [nucl-th].
- [8] G. Aad *et al.* (ATLAS), *Phys. Rev.* **C86**, 014907 (2012), arXiv:1203.3087 [hep-ex].
- [9] H. Song, S. A. Bass, U. Heinz, T. Hirano, and C. Shen, *Phys. Rev. Lett.* **106**, 192301 (2011), [Erratum: *Phys. Rev. Lett.* 109, 139904 (2012)], arXiv:1011.2783 [nucl-th].
- [10] B. Alver *et al.* (PHOBOS), *Phys. Rev.* **C77**, 014906 (2008), arXiv:0711.3724 [nucl-ex].
- [11] B. Alver *et al.* (PHOBOS), *Phys. Rev.* **C81**, 034915 (2010), arXiv:1002.0534 [nucl-ex].
- [12] J.-Y. Ollitrault, A. M. Poskanzer, and S. A. Voloshin, *Phys. Rev. C* **80**, 014904 (2009), arXiv:0904.2315 [nucl-ex].
- [13] K. Dusling, G. D. Moore, and D. Teaney, *Phys. Rev. C* **81**, 034907 (2010), arXiv:0909.0754 [nucl-th].
- [14] R. A. Lacey, A. Taranenko, R. Wei, N. Ajitanand, J. Alexander, *et al.*, *Phys. Rev.* **C82**, 034910 (2010), arXiv:1005.4979 [nucl-ex].
- [15] C. Shen, U. Heinz, P. Huovinen, and H. Song, *Phys. Rev. C* **84**, 044903 (2011), arXiv:1105.3226 [nucl-th].
- [16] H. Niemi, G. S. Denicol, H. Holopainen, and P. Huovinen, *Phys. Rev.* **C87**, 054901 (2013), arXiv:1212.1008 [nucl-th].
- [17] J. Fu, *Phys. Rev.* **C92**, 024904 (2015).
- [18] M. Abdallah *et al.* (STAR), *Phys. Rev. Lett.* **129**, 252301 (2022), arXiv:2201.10365 [nucl-ex].
- [19] J. Adam *et al.* (STAR), *Phys. Lett.* **B783**, 459 (2018), arXiv:1803.03876 [nucl-ex].
- [20] J. Adam *et al.* (ALICE), *Phys. Rev. Lett.* **117**, 182301 (2016), arXiv:1604.07663 [nucl-ex].
- [21] Z. Qiu and U. W. Heinz, *Phys. Rev. C* **84**, 024911 (2011), arXiv:1104.0650 [nucl-th].
- [22] A. Adare *et al.* (PHENIX), *Phys. Rev. Lett.* **107**, 252301 (2011), arXiv:1105.3928 [nucl-ex].
- [23] N. Magdy (STAR), *Proceedings, 27th International Conference on Ultrarelativistic Nucleus-Nucleus Collisions (Quark Matter 2018): Venice, Italy, May 14-19, 2018*, *Nucl. Phys.* **A982**, 255 (2019), arXiv:1807.07638 [nucl-ex].
- [24] L. Adamczyk *et al.* (STAR), *Phys. Rev. C* **94**, 034908 (2016), arXiv:1601.07052 [nucl-ex].
- [25] L. Adamczyk *et al.* (STAR), *Phys. Rev. C* **93**, 014907 (2016), arXiv:1509.08397 [nucl-ex].
- [26] L. Adamczyk *et al.* (STAR), *Phys. Rev. Lett.* **115**, 222301 (2015).
- [27] L. Adamczyk *et al.* (STAR), *Phys. Rev. Lett.* **116**, 112302 (2016), arXiv:1601.01999 [nucl-ex].
- [28] J. Adam *et al.* (STAR), *Phys. Rev. Lett.* **122**, 172301 (2019), arXiv:1901.08155 [nucl-ex].
- [29] F. G. Gardim, J. Noronha-Hostler, M. Luzum, and F. Grassi, *Phys. Rev.* **C91**, 034902 (2015), arXiv:1411.2574 [nucl-th].
- [30] H. Holopainen, H. Niemi, and K. J. Eskola, *Phys. Rev.* **C83**, 034901 (2011), arXiv:1007.0368 [hep-ph].
- [31] G.-Y. Qin, H. Petersen, S. A. Bass, and B. Muller, *Phys. Rev. C* **82**, 064903 (2010), arXiv:1009.1847 [nucl-th].
- [32] C. Gale, S. Jeon, B. Schenke, P. Tribedy, and R. Venugopalan, *Phys. Rev. Lett.* **110**, 012302 (2013), arXiv:1209.6330 [nucl-th].
- [33] K. M. Burke *et al.* (JET), *Phys. Rev. C* **90**, 014909 (2014), arXiv:1312.5003 [nucl-th].
- [34] P. Liu and R. A. Lacey, *Phys. Rev. C* **98**, 021902 (2018), arXiv:1802.06595 [nucl-ex].
- [35] K. Adcox *et al.* (PHENIX), *Phys. Rev. Lett.* **88**, 022301 (2002), arXiv:nucl-ex/0109003.
- [36] C. Adler *et al.* (STAR), *Phys. Rev. Lett.* **89**, 202301 (2002), arXiv:nucl-ex/0206011.
- [37] H.-z. Zhang, J. F. Owens, E. Wang, and X. N. Wang, *J. Phys. G* **35**, 104067 (2008), arXiv:0804.2381 [hep-ph].
- [38] B. Abelev *et al.* (ALICE), *JHEP* **03**, 013 (2014), arXiv:1311.0633 [nucl-ex].

- [39] Y. Mehtar-Tani, J. G. Milhano, and K. Tywoniuk, *Int. J. Mod. Phys. A* **28**, 1340013 (2013), arXiv:1302.2579 [hep-ph].
- [40] G.-Y. Qin and X.-N. Wang, *Int. J. Mod. Phys. E* **24**, 1530014 (2015), arXiv:1511.00790 [hep-ph].
- [41] B. H. Alver, C. Gombeaud, M. Luzum, and J.-Y. Ollitrault, *Phys. Rev. C* **82**, 034913 (2010), arXiv:1007.5469 [nucl-th].
- [42] H. Petersen, G.-Y. Qin, S. A. Bass, and B. Muller, *Phys. Rev. C* **82**, 041901 (2010), arXiv:1008.0625 [nucl-th].
- [43] R. A. Lacey, R. Wei, N. N. Ajitanand, and A. Taranenko, *Phys. Rev. C* **83**, 044902 (2011), arXiv:1009.5230 [nucl-ex].
- [44] D. Teaney and L. Yan, *Phys. Rev. C* **83**, 064904 (2011), arXiv:1010.1876 [nucl-th].
- [45] H. Niemi, K. J. Eskola, and R. Paatelainen, *Phys. Rev. C* **93**, 024907 (2016), arXiv:1505.02677 [hep-ph].
- [46] J. Noronha-Hostler, L. Yan, F. G. Gardim, and J.-Y. Ollitrault, *Phys. Rev. C* **93**, 014909 (2016), arXiv:1511.03896 [nucl-th].
- [47] M. D. Sievert and J. Noronha-Hostler, *Phys. Rev. C* **100**, 024904 (2019), arXiv:1901.01319 [nucl-th].
- [48] S. Rao, M. Sievert, and J. Noronha-Hostler, *Phys. Rev. C* **103**, 034910 (2021), arXiv:1910.03677 [nucl-th].
- [49] B. Schenke, S. Jeon, and C. Gale, *Phys. Lett. B* **702**, 59 (2011), arXiv:1102.0575 [hep-ph].
- [50] P. Bozek, *Phys. Rev. C* **85**, 034901 (2012), arXiv:1110.6742 [nucl-th].
- [51] F. G. Gardim, F. Grassi, M. Luzum, and J.-Y. Ollitrault, *Phys. Rev. Lett.* **109**, 202302 (2012), arXiv:1203.2882 [nucl-th].
- [52] T. Hirano, P. Huovinen, K. Murase, and Y. Nara, *Prog. Part. Nucl. Phys.* **70**, 108 (2013), arXiv:1204.5814 [nucl-th].
- [53] J. E. Bernhard, J. S. Moreland, S. A. Bass, J. Liu, and U. Heinz, *Phys. Rev. C* **94**, 024907 (2016), arXiv:1605.03954 [nucl-th].
- [54] J. E. Bernhard, J. S. Moreland, and S. A. Bass, *Nature Phys.* **15**, 1113 (2019).
- [55] J. S. Moreland, J. E. Bernhard, and S. A. Bass, *Phys. Rev. C* **101**, 024911 (2020), arXiv:1808.02106 [nucl-th].
- [56] D. Everett *et al.* (JETSCAPE), *Phys. Rev. Lett.* **126**, 242301 (2021), arXiv:2010.03928 [hep-ph].
- [57] D. Everett *et al.* (JETSCAPE), *Phys. Rev. C* **103**, 054904 (2021), arXiv:2011.01430 [hep-ph].
- [58] G. Nijs, W. van der Schee, U. Gürsoy, and R. Snellings, *Phys. Rev. C* **103**, 054909 (2021), arXiv:2010.15134 [nucl-th].
- [59] J. Auvinen, K. J. Eskola, P. Huovinen, H. Niemi, R. Paatelainen, and P. Petreczky, *Phys. Rev. C* **102**, 044911 (2020), arXiv:2006.12499 [nucl-th].
- [60] J. E. Parkkila, A. Onnerstad, and D. J. Kim, *Phys. Rev. C* **104**, 054904 (2021), arXiv:2106.05019 [hep-ph].
- [61] A. V. Giannini, M. N. Ferreira, M. Hippert, D. D. Chinellato, G. S. Denicol, M. Luzum, J. Noronha, T. Nunes da Silva, and J. Takahashi (ExTREMe), *Phys. Rev. C* **107**, 044907 (2023), arXiv:2203.17011 [nucl-th].
- [62] M. Luzum and J.-Y. Ollitrault, *Nucl. Phys. A* **904-905**, 377c (2013), arXiv:1210.6010 [nucl-th].
- [63] G. S. Denicol, C. Gale, S. Jeon, J. F. Paquet, and B. Schenke, (2014), arXiv:1406.7792 [nucl-th].
- [64] C. Shen, Z. Qiu, and U. Heinz, *Phys. Rev. C* **92**, 014901 (2015), arXiv:1502.04636 [nucl-th].
- [65] R. S. Bhalerao, A. Jaiswal, and S. Pal, *Phys. Rev. C* **92**, 014903 (2015), arXiv:1503.03862 [nucl-th].
- [66] C. Loizides, *Phys. Rev. C* **94**, 024914 (2016), arXiv:1603.07375 [nucl-ex].
- [67] F. Gelis, G. Giacalone, P. Guerrero-Rodríguez, C. Marquet, and J.-Y. Ollitrault, (2019), arXiv:1907.10948 [nucl-th].
- [68] P. Carzon, S. Rao, M. Luzum, M. Sievert, and J. Noronha-Hostler, *Phys. Rev. C* **102**, 054905 (2020), arXiv:2007.00780 [nucl-th].
- [69] R. Snyder, M. Byres, S. H. Lim, and J. L. Nagle, *Phys. Rev. C* **103**, 024906 (2021), arXiv:2008.08729 [nucl-th].
- [70] B. G. Zakharov, *JETP Lett.* **112**, 393 (2020), arXiv:2008.07304 [nucl-th].
- [71] J.-B. Rose, J.-F. Paquet, G. S. Denicol, M. Luzum, B. Schenke, S. Jeon, and C. Gale, *Nucl. Phys. A* **931**, 926 (2014), arXiv:1408.0024 [nucl-th].
- [72] S. Plumari, G. L. Guardo, F. Scardina, and V. Greco, *Phys. Rev. C* **92**, 054902 (2015), arXiv:1507.05540 [hep-ph].
- [73] P. Alba, V. Mantovani Sarti, J. Noronha, J. Noronha-Hostler, P. Parotto, I. Portillo Vazquez, and C. Ratti, *Phys. Rev. C* **98**, 034909 (2018), arXiv:1711.05207 [nucl-th].
- [74] A. Majumder, B. Muller, and X.-N. Wang, *Phys. Rev. Lett.* **99**, 192301 (2007), arXiv:hep-ph/0703082.
- [75] P. Staig and E. Shuryak, *Phys. Rev. C* **84**, 034908 (2011), arXiv:1008.3139 [nucl-th].
- [76] S. S. Gubser and A. Yarom, *Nucl. Phys. B* **846**, 469 (2011), arXiv:1012.1314 [hep-th].
- [77] R. A. Lacey, Y. Gu, X. Gong, D. Reynolds, N. N. Ajitanand, J. M. Alexander, A. Mwai, and A. Taranenko, (2013), arXiv:1301.0165 [nucl-ex].
- [78] M. Aaboud *et al.* (ATLAS), *Eur. Phys. J. C* **78**, 997 (2018), arXiv:1808.03951 [nucl-ex].
- [79] S. Acharya *et al.* (ALICE), *JHEP* **07**, 103 (2018), arXiv:1804.02944 [nucl-ex].
- [80] S. Acharya *et al.* (ALICE), *Phys. Lett. B* **784**, 82 (2018), arXiv:1805.01832 [nucl-ex].
- [81] K. Aamodt *et al.* (ALICE), *Phys. Rev. Lett.* **106**, 032301 (2011), arXiv:1012.1657 [nucl-ex].
- [82] J. Adam *et al.* (ALICE), *Phys. Rev. Lett.* **116**, 222302 (2016), arXiv:1512.06104 [nucl-ex].
- [83] S. Acharya *et al.* (ALICE), *Phys. Lett. B* **790**, 35 (2019), arXiv:1805.04432 [nucl-ex].
- [84] A. M. Sirunyan *et al.* (CMS), *Phys. Lett. B* **799**, 135049 (2019), arXiv:1902.03603 [hep-ex].
- [85] M. L. Miller, K. Reygers, S. J. Sanders, and P. Steinberg, *Ann. Rev. Nucl. Part. Sci.* **57**, 205 (2007), arXiv:nucl-ex/0701025.
- [86] B. Alver *et al.* (PHOBOS), *Phys. Rev. Lett.* **98**, 242302 (2007), arXiv:nucl-ex/0610037.
- [87] K. Tsukada *et al.*, *Phys. Rev. Lett.* **118**, 262501 (2017), arXiv:1703.04278 [nucl-ex].